



# GIS-based slope-adjusted curve number methods for runoff estimation

Elham Forootan

Received: 1 August 2022 / Accepted: 20 February 2023 / Published online: 20 March 2023  
© The Author(s), under exclusive licence to Springer Nature Switzerland AG 2023

**Abstract** Accurate estimation of surface runoff and determination of susceptible lands to runoff generation in ungauged watersheds were the problems for hydrologic engineering which could be predicted through a simple model such as Soil Conservation Service Curve Number (SCS-CN). Due to the slope effects on this method, slope adjustment for curve number was developed to improve its precision. So, the main objectives of this study were to apply GIS-based slope SCS-CN approaches for surface runoff estimation and compare the accuracy of three slope-adjusted models including: (a) model with three empirical parameters, (b) model with two parameters slope function, and (c) model with one parameter in the region located in the central part of Iran. For this purpose, soil texture, hydrologic soil group, land use, slope, and daily rainfall volume maps were utilized. In order to provide the curve number map of the study area, land use and hydrologic soil group layers built in Arc-GIS were intersected and the curve number was determined. Then, three slope adjustment equations were used to modify curve numbers of AMC-II by employing slope map. Finally, recorded runoff data of the hydrometric station were applied to assess the performance of the models through four statistical indicators of the root mean square error (RMSE), the Nash–Sutcliffe efficiency ( $E$ ), the coefficient of determination ( $R^2$ ), and percent bias (PB). Land use map analysis showed that rangeland was the dominant land use, whereas the soil

texture map specified the greatest and smallest area belonging to loam and sandy loam textures, respectively. Although the runoff results showed the overestimation of large rainfall values and underestimation for rainfall with less than 40 mm volume in both models, the values of  $E$  (0.78), RMSE (2), PB (16), and  $R^2$  (0.88) revealed that eq. (a) with three empirical parameters was the most accurate equation. The maximum percent of runoff generated by rainfall for eqs. (a), (b), and (c) were 68.43, 67.28, and 51.57% which showed that bareland located in south part with the slope of more than 5% was susceptible to runoff generation and should be paid attention to watershed management.

**Keywords** GIS · Slope-adjusted curve number · Runoff · Model accuracy

## Introduction

Accurate estimation of surface runoff which is known as rainfall runs toward the watershed outlet is one of the problems for water resource management and hydrologic engineering in ungauged watersheds (Bhuyan et al., 2022; Deshmukh et al., 2013; Soulis, 2021; Verma et al., 2017). It could be predicted through the well-documented and simple method of Soil Conservation Service Curve Number (USDA, 1986; SCS 1993; Verma et al., 2017). This method was based on initial abstraction and soil storage capacity parameters in a single entity named as curve number (CN) (Mishra et al., 2005). Hence, the curve number tables were designed according to hydrologic soil group (HSG), land use/cover, and

E. Forootan (✉)  
Department of Agriculture, Payame Noor University,  
Tehran, Iran  
e-mail: e.forotan@pnu.ac.ir

antecedent soil moisture condition (AMC) parameters for a slope of 5% (Hawkins Richard, 2014; Nazif et al., 2022). In this table, curve number (CN) was defined as a dimensionless index which varied from 0 to 100 theoretically (Verma et al., 2017) and could be applied for runoff estimation. Antecedent moisture condition, as the indicator, showed the effect of soil moisture status on runoff generation. In this regard, according to rainfall values of the previous 5 days and season, three AMC conditions (I, II, and III) were defined in this approach.

However, in situations with measured data, CNs could be determined according to the observed rainfall-runoff relationships (Ajmal et al., 2015; Farran & Elfeki, 2020; Ibrahim et al., 2022; Soulis & Valiantzas, 2013; Verma et al., 2022).

Although this approach was convenient and widely applied, it has some limitations which cause several modifications for this model (SCS, 1985, 1993, 2004). For instance, there was not a flexible guidance for determining antecedent moisture condition, and also the factors of rainfall properties and slope parameter were not considered in this approach (Huang et al., 2006; Singh et al., 2015). Slope is the parameter which affects this model through the decrease in initial abstraction, infiltration, and overland flow recession time (Chaplot & Le Bissonnais, 2003; Chaudhary et al., 2013; Ebrahimian et al., 2012; Evett et al., 1985; Fang et al., 2008; Jha et al., 2014; Philip, 1991). Several researches have shown the underestimated prediction in the steep-slope watersheds using this approach (Sharpley & Williams, 1990; Ajmal et al., 2016; Shi & Wang, 2020; Sharma et al., 2022).

In this regard, slope adjustment for curve number was applied to improve runoff estimation (Ajmal et al., 2016, 2020; Huang et al., 2006; Mishra et al., 2014; Sharpley & Williams, 1990; Williams & Izaurralde, 2005; Williams et al., 2012). Sharpley and Williams (1990) suggested the first slope-corrected curve number equation with three empirical parameters ( $a$ ,  $b$ , and  $c$ ) which could not be tested well. Huang et al. (2006) introduced and verified the equation with two empirical parameters ( $a_1$  and  $a_2$ ) for slope gradients on the Loess Plateau of China. Ajmal et al. (2020) applied a slope-adjusted CN method with one parameter ( $b$ ) in steep-slope watersheds which the results verified the precision of the proposed method. As mentioned above, several equations have been presented by the different researchers such as Sharpley and Williams (1990),

Huang et al. (2006), and Ajmal et al. (2020) which comparing their accuracy in various conditions can lead to specify the most precise equation.

In addition to runoff estimation problem, the specification of susceptible lands to runoff generation is another subject in water resource planning. The combination of GIS and RS with SCS-CN model solved this problem (Rajbanshi, 2016) for different climatic conditions and land uses (Soulis & Valiantzas, 2013; Verma et al., 2017). Various studies verified the accuracy of employing GIS and RS tools for this purpose (Nayak & Jaiswal, 2003, Zhan & Huang 2004, Geena & Ballukraya, 2011, Gitika & Ranjan, 2014; Al-Ghobari et al., 2020; Mahmood et al., 2020; Yousuf et al., 2022; Gupta & Dixit, 2022). Also, Verma et al. (2022) revealed the capability of GIS-based NRCS-CN method to present the characteristics of the watershed and actual precipitation. It is obvious that the watershed located in arid and semi-arid climate would confront with droughts and water crisis problems due to a lack of water resources which predicting precise runoff volume and specifying sensitive lands to runoff generation cause proper surface water management.

So, this research is an empirical contribution type with two main objectives: (1) to apply GIS-based slope SCS-CN approaches for spatial and temporal hydrological parameters estimation and (2) to compare the accuracy of three slope-adjusted models.

## Material and methods

### Study area

For employing these approaches, the watershed which lies between  $50^{\circ} 04' - 50^{\circ} 28' E$ ,  $34^{\circ} 28' - 34^{\circ} 44' N$  with  $510.07 \text{ km}^2$  area was selected (Fig. 1). This region, located in the central part of Iran, with an average annual rainfall of 170 mm was classified as an arid region according to De Marton climate categorization (Forootan, 2019). There are some villages where their rural people utilize river water for irrigation of orchards and cultivated land. The discharge rate of the main river, with 11.61 km in length, was measured at Tagharood hydrometric station located at the watershed outlet. There is not any climatic station in the region. Therefore, the statistics of three climatic stations named Aghalak, Salarieh, and 15 Khordad Dam located around the watershed were

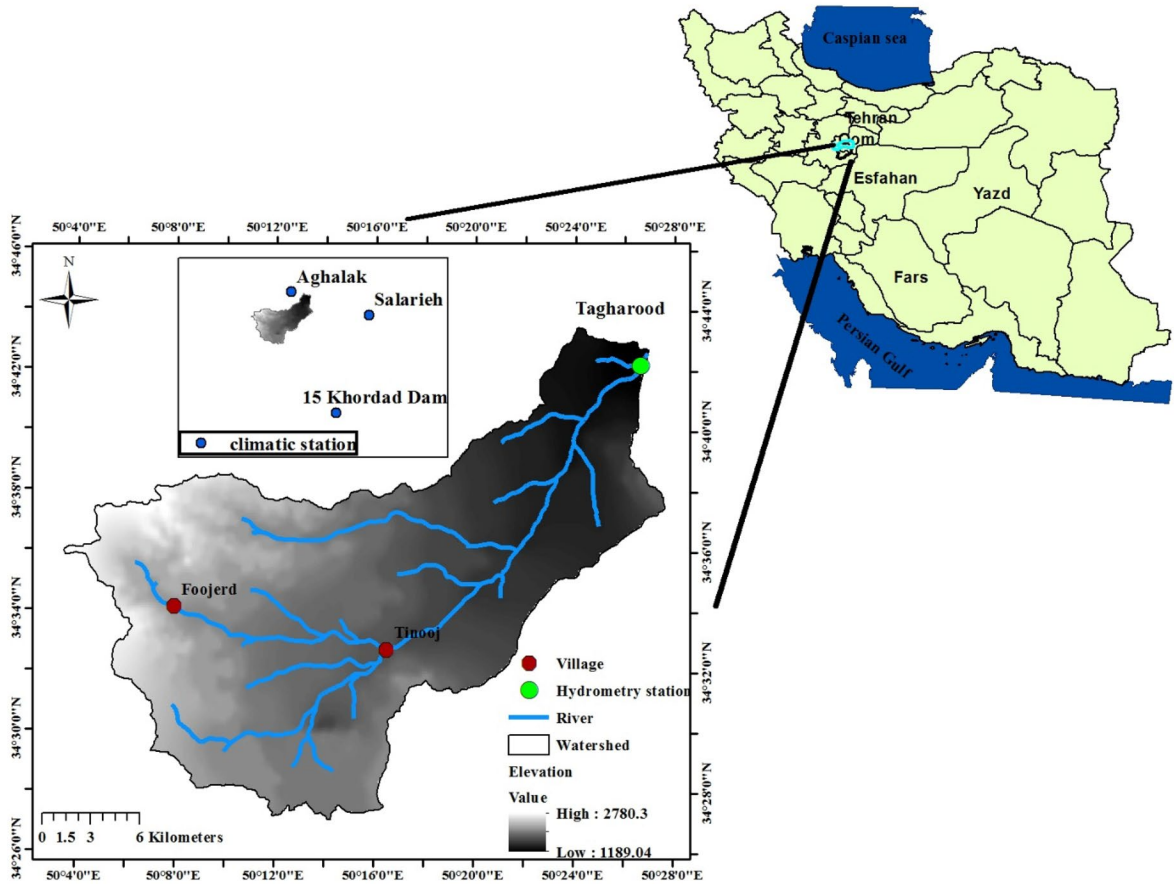


**Fig. 1** Location of the study area

considered in this study (Fig. 1). Thus, the statistics of all climatic and hydrometric stations were collected from Iran Water Resources Management Company for 2005–2013.

**Methodology**

In this research, three proposed equations of slope-adjusted  $CN_{II}$  were employed to calculate runoff volume in Arc-GIS environment while the results were compared to observed runoff through statistical analysis. The overall methodology of the study was depicted in Fig. 2. For this goal, different maps were prepared as the following:

*Soil texture*

The soil texture is the key parameter for determining hydrologic soil group (Saxton et al., 1986; Wood &

Blackburn, 1984). The soil map of the watershed was prepared using soil profile data up to 100 cm depth from the Food and Agriculture Organization database. It includes a soil texture raster layer classified using a soil texture triangle based on the USDA classification (USDA, 1987). The spatial accuracy of the layer is 250 m of pixel size.

*Hydrologic soil group (HSG)*

The hydrologic soil group describes the soil infiltration potential after prolonged wetting conditions (Willard, 2010). Soils without any protected vegetation which receive long-duration rainfall and meet wet conditions were classified as one of four groups (A, B, C, and D) on the basis of the water infiltration rate. Soils in group A were characterized by sand textures and low runoff potential in wet condition, whereas group B soils were specified with loamy sand or

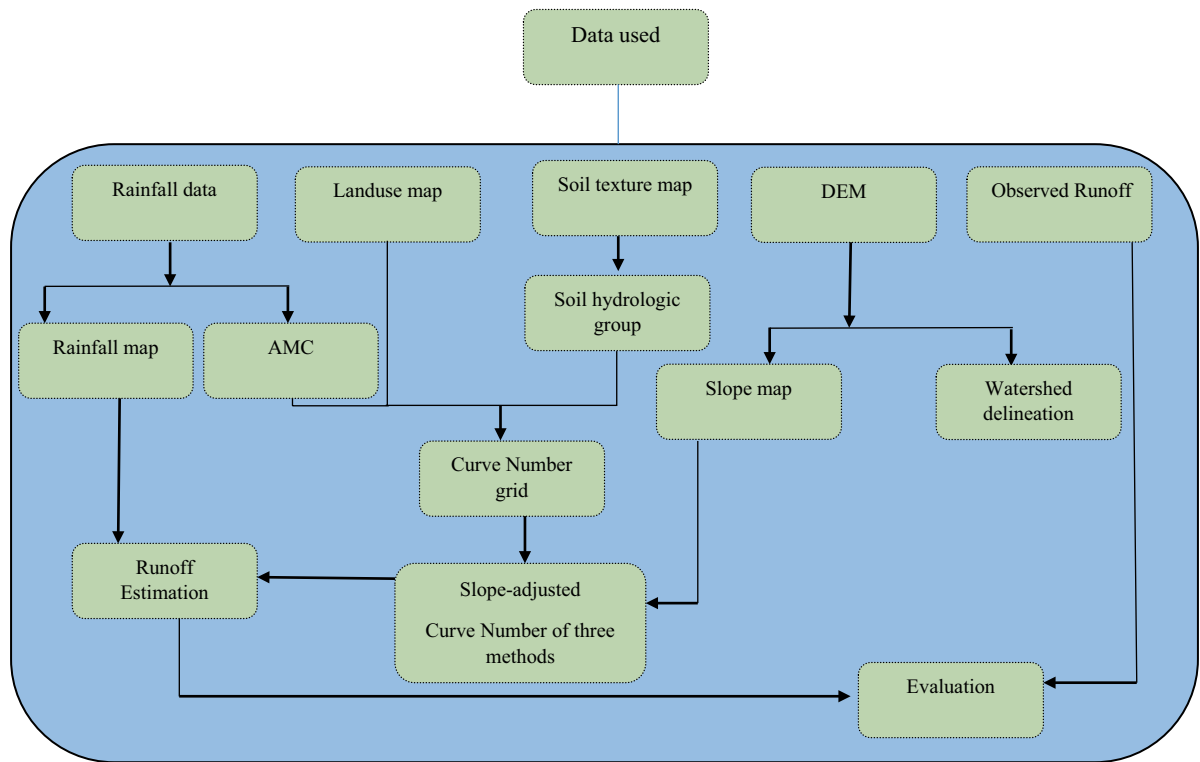


**Fig. 2** Methodology flow chart applied in this study

sandy loam textures and moderately low potential for runoff generation. Generally, soils with moderately low runoff potential which have clay, sandy clay, or silty clay textures may be classified in group C. However, the soils with less than 50% sand, more than 40% clay, which have clayey textures and high runoff potential could be known as group D (Werner et al., 2007). The infiltration rates in hydrologic soil groups decrease from A to D (Al-Ghobari et al., 2020).

*Land use/land cover (LULC)*

Land use/land cover properties which affect runoff volume need to be used in SCS curve number determination. So, the classified land use map of the study area provided by Natural Resource and Watershed Management Department of Qom province (2010) was applied for this study.

*Slope*

Steeper slope gradients cause more runoff production capacity due to larger flow velocities and lesser

water infiltration (Fang et al., 2008). For this purpose, the digitized contour lines of topographic map with 1:50,000 scale, provided by Iran Survey Organization, were interpolated to derive digital elevation model (DEM) with a 418 × 418-m pixel size. Then, constructed DEM was utilized for slope map provision through Spatial Analyst in Arc-GIS 10.2.

*Rainfall*

The spatial distribution maps of the maximum daily rainfall were provided by applying IDW method in Arc-GIS.10.2. In this method, the interpolated values were determined through recoded rainfall data from four nearby stations. So, ten recorded rainfall events at nearby stations from 2005 to 2013 were applied for this purpose.

Curve number model and slope-adjusted  $CN_{II}$ . The SCS runoff could be calculated as following:

$$Q = \begin{cases} \frac{(P-\lambda S)^2}{P+(1-\lambda)S} & (P > \lambda S) \\ 0 & (P \leq \lambda S) \end{cases} \quad (1)$$

$$S = \left(\frac{25400}{CN} - 254\right) \tag{2}$$

where  $Q$ =runoff depth (mm), $\lambda$  = initial abstraction taken as 0.2S,  $P$ =cumulative rainfall volume (mm),  $S$ =maximum potential water retention volume (mm), and  $CN$ =curve number. In this study, the  $CN_{II}$  for the condition of AMC-II was considered according to the antecedent moisture condition (AMC) classification presented in Table 1 (USDA, 1986). For providing curve number map of the study area, land use and hydrologic soil group layers built in Arc-GIS were intersected and the curve number of each unit was determined based on National engineering handbook (1972, 2004). Then, slope adjustment equations were used to modify curve number values because the slope values greater than 5% can be observed in 48.40% of the total area.

The curve number associated with normal condition (AMC-II) could be converted into  $CN_I$  and  $CN_{III}$  of (AMC-I) and (AMC-III) conditions as following:

$$CN_I = \frac{4.2 \times CN_{II}}{10 - (0.058 \times CN_{II})} \tag{3}$$

$$CN_{III} = \frac{23 \times CN_{II}}{10 + (0.13 \times CN_{II})} \tag{4}$$

So, slope adjustment equations for  $CN$  prediction were taken as below:

(a) Model with three empirical parameter values of  $a = \frac{1}{3}$ ,  $b = 2$ ,  $c = -13.86$  (Sharpley & Williams, 1990):

$$CN_{II\alpha} = a(CN_{III} - CN_{II})(1 - be^{-c\alpha}) + CN_{II} = \frac{(CN_{III} - CN_{II})}{3} (1 - 2e^{-13.86\alpha}) + CN_{II} \tag{5}$$

(b) Model with two parameter slope function values of  $a_1 = 323.57$ ,  $a_2 = 15.63$  (Huang et al., 2006):

$$CN_{II\alpha} = CN_{II} \left( \frac{a_1 + a_2(\alpha - 0.5)}{(\alpha - 0.5) + a_1} \right) = CN_{II} \left( \frac{322.79 + 15.63\alpha}{\alpha + 323.52} \right) \tag{6}$$

(c) Model with one parameter value of  $b = 7.125$  (Ajmal et al., 2020):

$$CN_{II\alpha} = \left[ \frac{CN_{III} - CN_{II}}{2} \right] \times [1 - e^{-b(\alpha-0.05)}] + CN_{II} = \left[ \frac{CN_{II}(50 - 0.5CN_{II})}{CN_{II} + 75.43} \right] \times [1 - e^{-7.125(\alpha-0.05)}] + CN_{II} \tag{7}$$

where  $\alpha$  is average slope of watershed in m/m. The slope-adjusted  $CN_{II}$  maps for three equations were provided in Raster Calculator of Arc-GIS through employing the region slope map. Then, the provided maps were used to calculate runoff values based on eqs. (1) and (2). Finally, the average runoff value of each rainfall event was estimated through the reclassified map of runoff as following:

$$R_{me} = \frac{\sum (R_i \times A_i)}{A_t} \tag{8}$$

where  $R_{me}$  = mean estimated daily runoff value,  $R_i$ = estimated runoff value in each class,  $A_i$ = the area with runoff value of  $R_i$ , and  $A_t$  = the total watershed area.

Observed runoff in Tagharood station was calculated by eq. (9):

$$R_{mo} = \frac{Q_{md}}{A_t} \times 86.4 \tag{9}$$

$R_{mo}$  = recorded mean daily runoff (mm),  $Q_{md}$ = recorded mean daily flow ( $\frac{m^3}{s}$ ),  $A_t$ = the total watershed area ( $km^2$ ). It should be noted that some parts of the runoff directed to streams and rivers were utilized for irrigation before entering the watershed outlet. So, water consumption for agriculture was considered for calculating the total runoff of the watershed.

*Statistical analysis for model accuracy assessment*

Four statistical indicators of the root mean squares error (RMSE), the Nash–Sutcliffe efficiency ( $E$ ), the coefficient of determination ( $R^2$ ), and percent bias (PB) were applied to assess the degree of agreement between the observed and predicted runoff:

**Table 1** The classification of AMC condition

AMC	Total rainfall in previous 5 days	
	Dormant season	Growing season
I	Less than 12.7 mm	Less than 35.6
II	12.7 to 27.9 mm	35.6 to 53.3 mm
III	More than 27.9 mm	More than 53 mm



$$E = 1 - \left[ \frac{\sum_{i=1}^n (Q_{oi} - Q_{ei})^2}{\sum_{i=1}^n (Q_{oi} - \bar{Q}_o)^2} \right] \tag{10}$$

$$RMS = \sqrt{\frac{1}{n} \sum_{i=1}^n (Q_{oi} - Q_{ei})^2} \tag{11}$$

$$R^2 = \frac{\left[ \sum_{i=1}^n (Q_{ei} - \bar{Q}_e)(Q_{oi} - \bar{Q}_o) \right]^2}{\sum_{i=1}^n (Q_{ei} - \bar{Q}_e)^2 \sum_{i=1}^n (Q_{oi} - \bar{Q}_o)^2} \tag{12}$$

$$PB = \left[ \frac{\sum_{i=1}^n (Q_{oi} - Q_{ei})}{\sum_{i=1}^n (Q_{oi})} \right] \tag{13}$$

where  $Q_{oi}$ ,  $Q_{ei}$ ,  $\bar{Q}_o$ , and  $\bar{Q}_e$  = observed, predicted, the average of observed, and predicted runoff of each rainfall event, respectively.

Higher values of  $E$  and  $R^2$ , (optimum = 1) explain better prediction of the model. The  $E$  values equal or less than 0.5 indicate the unsatisfactory model results, whereas the values greater than 0.65, 0.8, and 0.9 show the satisfactory, good, and very good performance of the hydrologic model, respectively (Ritter & Muñoz-Carpena, 2013). Conversely, smaller values of RMSE (optimum = 0) describe better prediction of the model (Ajmal et al., 2016). For percent bias, the optimum value is equal to zero. Positive values of PB depict the underestimation, whereas the negative values show the overestimation bias of the model (Ajmal et al., 2020).

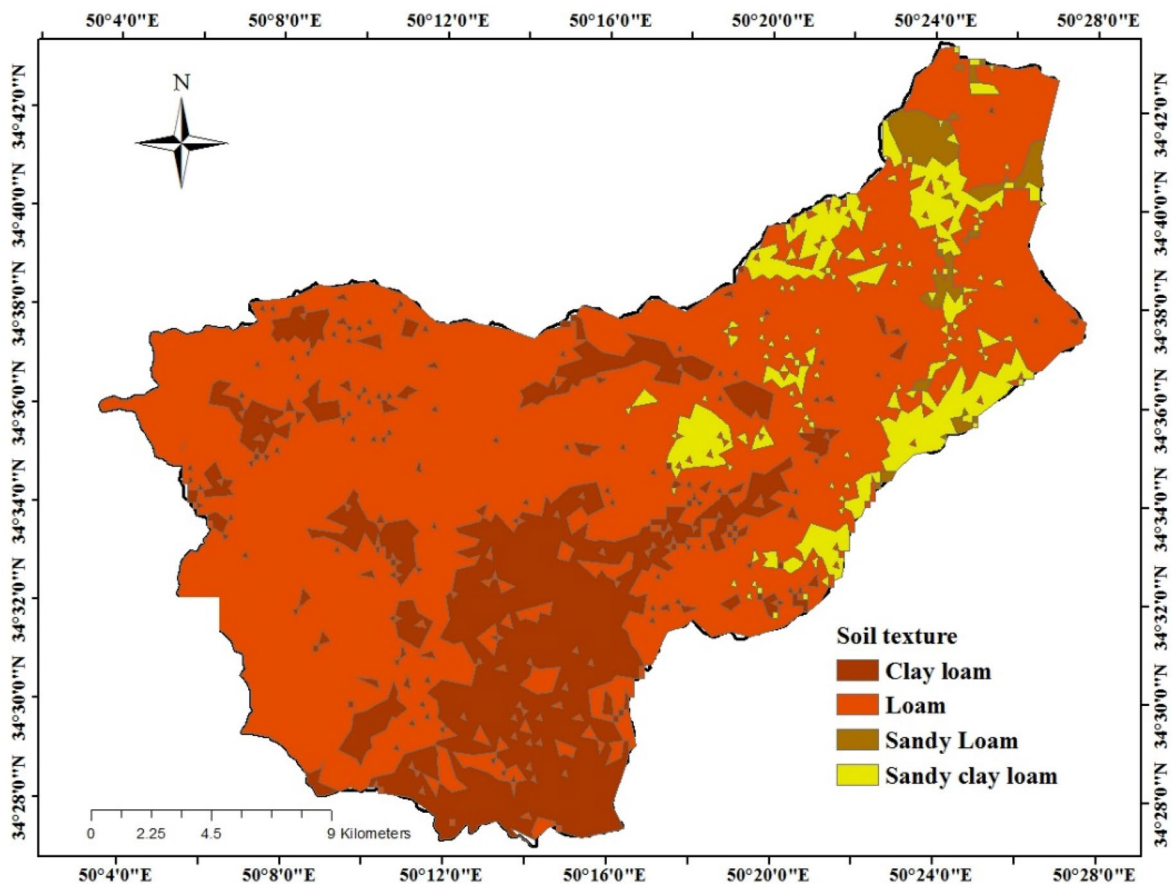


Fig. 3 Classified thematic map of soil texture of the study area

## Results

### Soil texture

Soil texture as one of the most important soil properties affects infiltration process and surface runoff generation. In this study, loam and clay loam were the dominant soil textures, which comprise 68.95 and 22.3% of the total area, respectively. Meanwhile, 7.13 and 1.62% was covered with sandy clay loam and sandy loam textures (Fig. 3).

### Hydrologic soil group

The hydrologic soil group (HSG) determination is the necessity for the curve numbers estimation (Auerswald & Gu, 2021). In this study, the HSG layer

was built through Arc-GIS 10.2 according to the soil texture map. As can be seen in Fig. 4, the percent areas of A, B, C, and D groups were 1.62%, 68.95%, 7.13%, and 22.3%, respectively. It could be observed that the greatest and smallest areas pertain to B and A groups, respectively (Fig. 4).

### Land use/land cover (LULC)

Vegetation cover removal causes high runoff volumes (Zhao et al., 2004). Accordingly, land use and land cover maps are important due to their impacts on hydrological processes (Gonzalez et al., 2015). In the region, rangeland as the dominant land use type comprises 77.21% of the total area, whereas 8.54 and 14.25% belong to agriculture and bareland, respectively (Fig. 5).

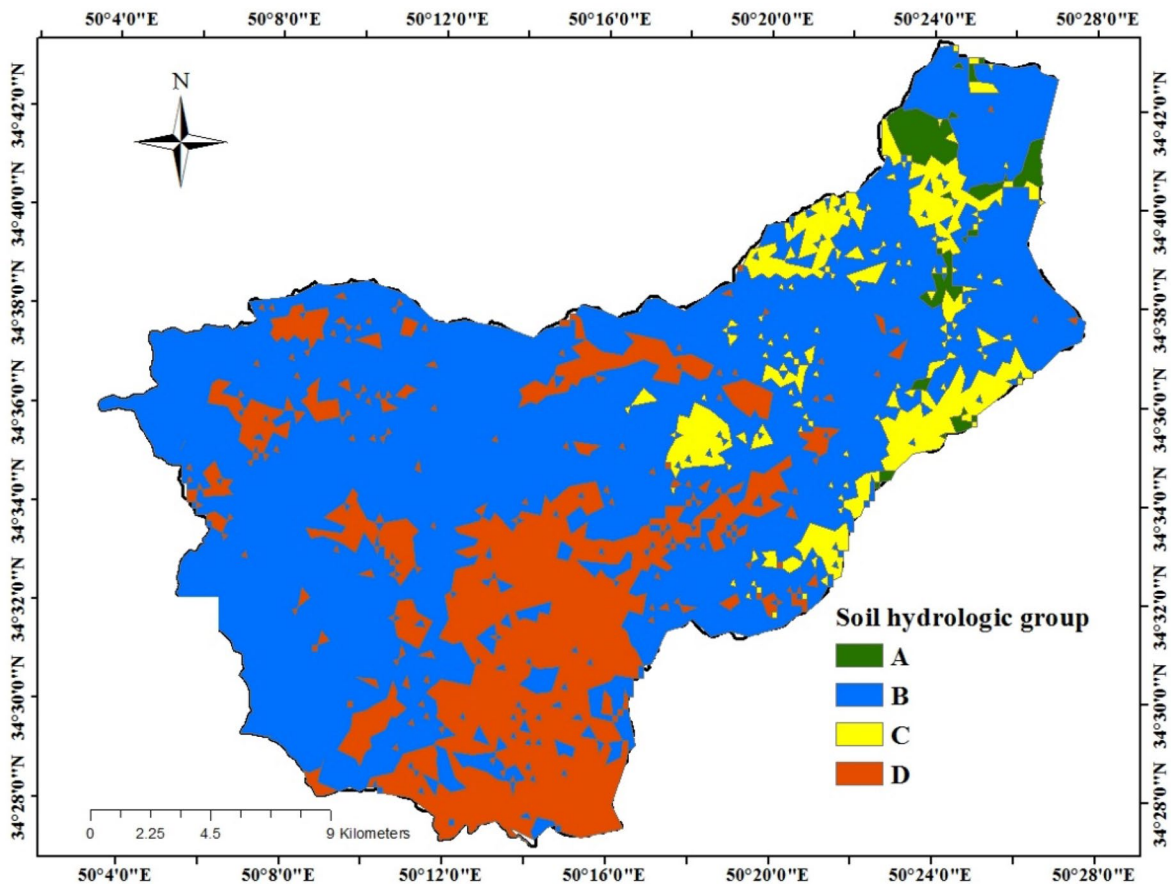


**Fig. 4** Hydrologic soil groups of the study area

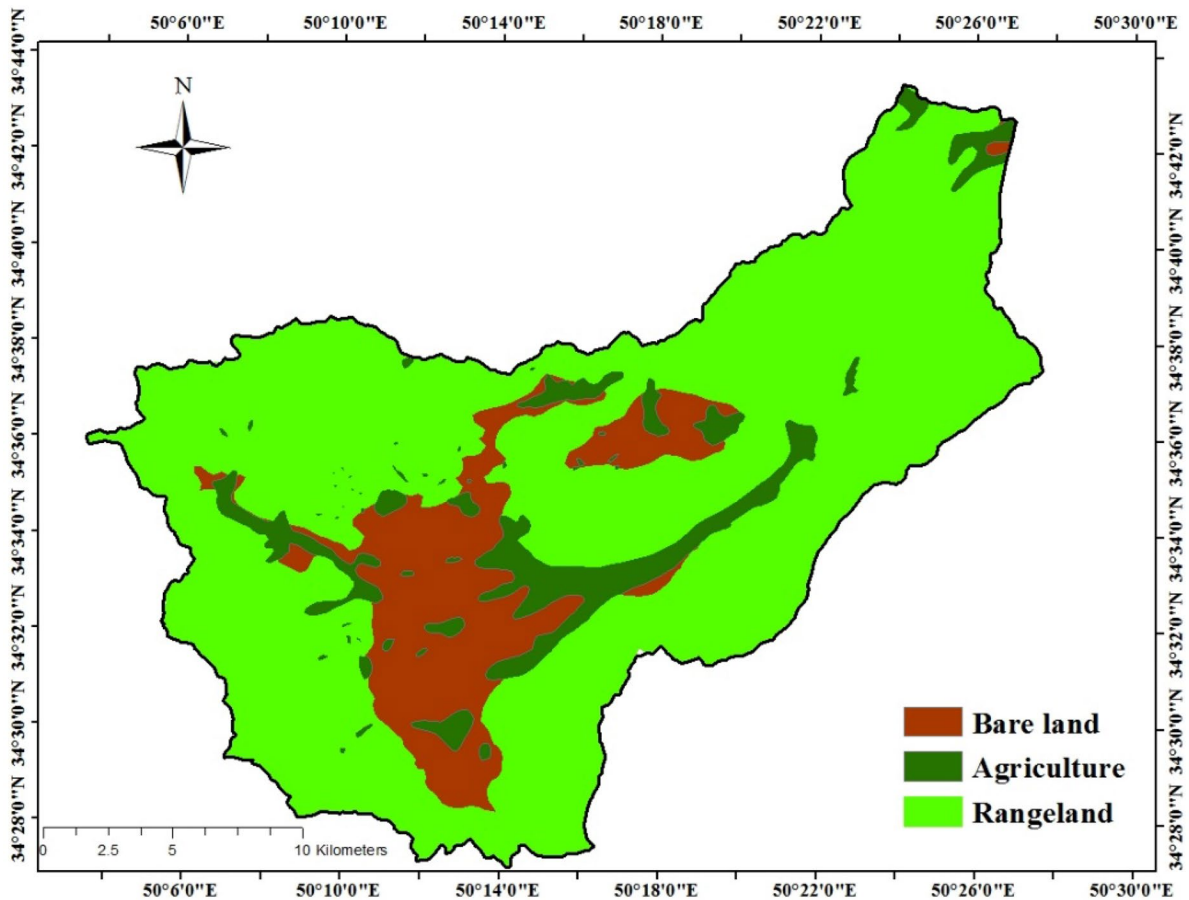


**Fig. 5** Land use classified thematic map

### Slope

Due to the higher potential of steep slopes for runoff generation (Fang et al., 2008), the slope percent of the study area was presented in Fig. 6. The classified slope map showed that the 0–5%, 5–15%, 15–30%, and 30–66% classes occupied 51.60%, 32.29%, 13.84%, and 2.27%, respectively. This categorization indicated that the greatest part of the watershed could be observed with 0–5% slope and the smallest part was assigned to the 30–66% class.

### Rainfall

Rainfall distribution maps of ten events were given in Fig. 7. This figure not only presented the decrease in rainfall volume from the north to south of the region in most cases (60%), but also indicated small

variations in some events. Except for the maximum range of rainfall volume variations that have occurred in 2007 (17.65 to 29 mm) and 2005 (36.28 to 46 mm), the other ranges were less than 9 mm (Table 2).

### SCS-curve number maps

SCS-CN value of each cell was provided by HSG, and LULC maps according to AMC-II. As can be observed in Fig. 8, original curve number values varied from 67 to 94. In the next step, the traditional  $CN_{II}$  values were modified by three equations to obtain slope-adjusted  $CN_{II}$ . Figure 8 showed that the highest slope-adjusted  $CN_{II}$  for the equations (a, b, and c) proposed by Sharpley and Williams (1990), Huang et al. (2006), and Ajmal et al. (2020) were 94.99, 95.82, and 95.66 attributed to bareland while the lowest slope-adjusted  $CN_{II}$  of these equations



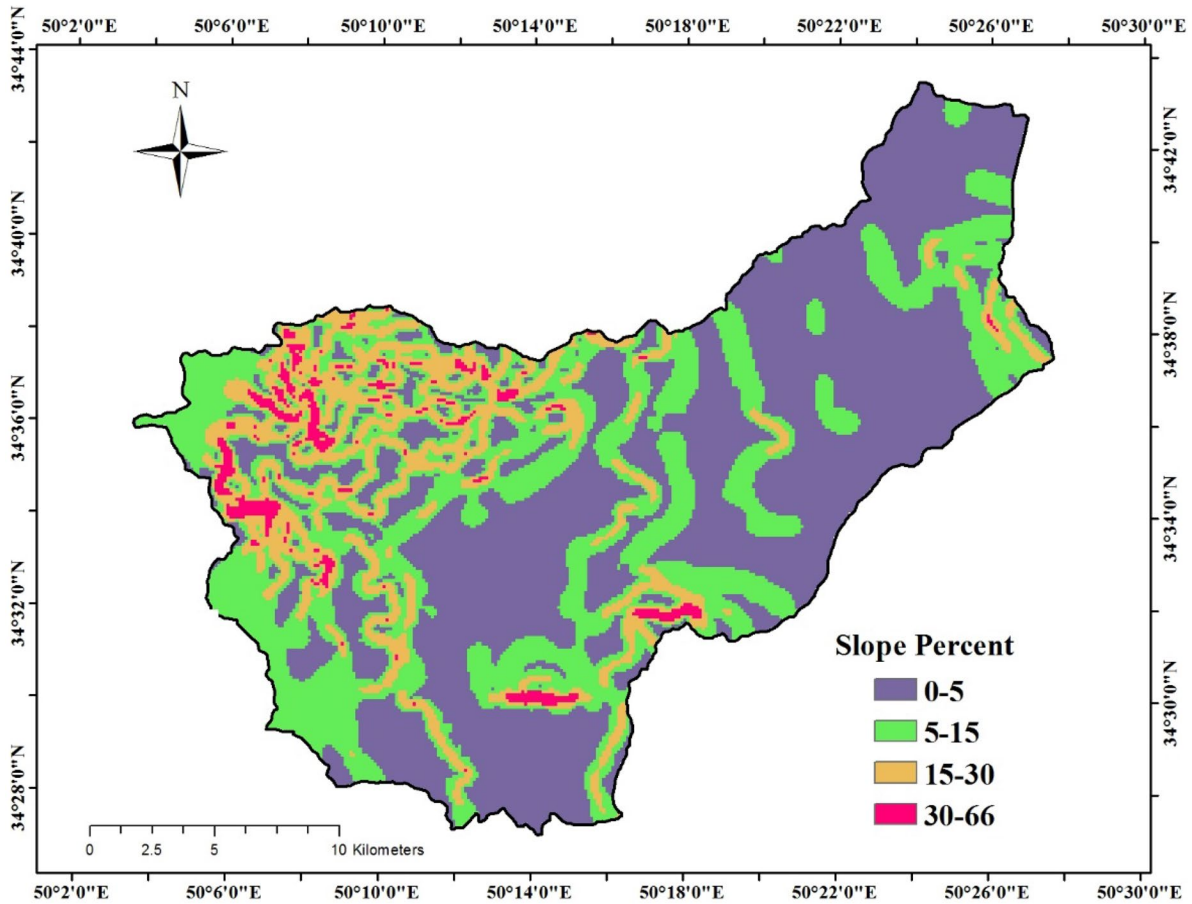


**Fig. 6** Slope classified thematic map

were 63.11, 66.9, and 74.76 found in rangeland and agricultural lands.

As could be seen in Table 3, the areas for the original  $CN_{II}$  classes of “less than 68”, “68–79”, “79–89,” and “89–100” were 1.6%, 60.85%, 31.37%, and 6.18%, respectively. These results showed that the “68–79” and “less than 68” classes occupied the greatest and the smallest parts of the watershed. Moreover, these finding indicated the highest and lowest potential maximum retention classes could be observed in 1.6% and 6.18% of the total area. Comparing traditional  $CN_{II}$  values with modified  $CN_{II}$  for Sharpley and Williams (eq. a) showed the decrease in the two classes area of “less than 68” and “68–79” (0.31 and 34.05%) and the increase for two groups areas of “79–89” and “89–100” (26.82 and 7.54%). For the  $CN_{II}$  results of Huang et al. (2006), named as

eq. (b), the comparison with conventional SCS-CN values revealed the decrease in the “68–79” class area (33.35%) as well as the increase in the classes’ areas of “79–89” and “89–100” (25.78 and 7.57%). Also, calculating the difference between the estimated  $CN_{II}$  of eq. (c), suggested by Ajmal et al. (2020), with the original  $CN_{II}$  values showed the reduction in two groups areas of “less than 68” and “68–79” (1.6 and 59.26%) as well as the increment in the areas covered with “79–89” and “89–100” classes (29.43 and 31.43%). It was found that the classes areas with more than 79 curve number values increased 34.36, 33.35, and 60.86% by employing three equations of Sharpley and Williams (1990), Huang et al. (2006), and Ajmal et al. (2020) which these changes explained the impacts of slope in reducing the potential maximum retention and ascending the runoff generation.

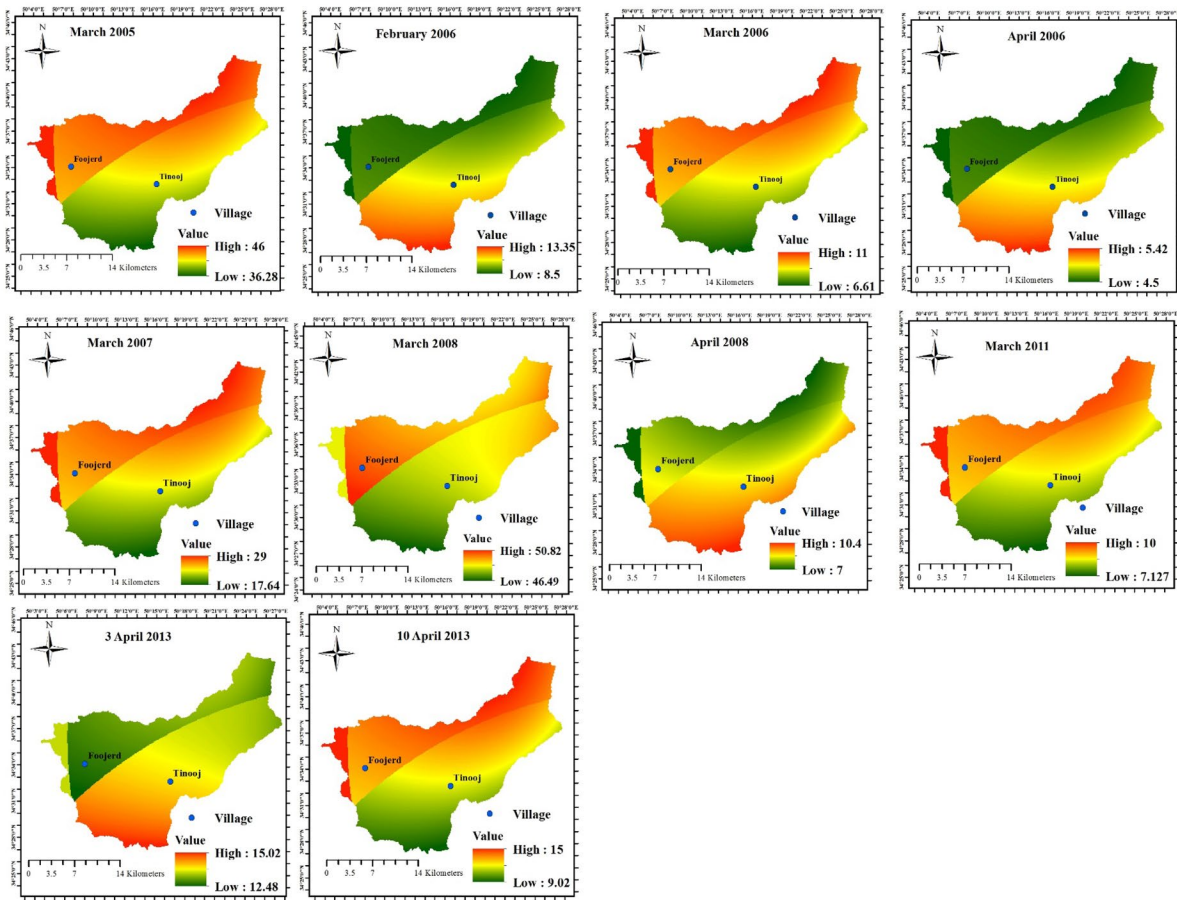


**Fig. 7** Rainfall distribution map of study area

Runoff of three slope-adjusted CNII methods

The spatial and temporal runoff maps originated from  $CN_{II}$  equations (a), (b), and (c) were presented

**Table 2** Variability of rainfall events

No	Month/year	Max value	Min value	Range (mm)
1	March/2005	46	36.28	9.72
2	February/2006	13.35	8.5	4.85
3	March/2006	11	6.61	4.39
4	April/2006	5.42	4.5	0.92
5	March/2007	29	17.65	11.35
6	March/2008	50.83	46.49	3.4
7	April/2008	10.4	7	4.34
8	March/2011	10	7.13	2.87
9	3April/2013	15.02	12.48	2.54
10	10April/2013	15	9.02	5.98

in Figs. 9, 10, and 11. In 2006 and 2008, so much of the watershed can be seen with low runoff generation (0) in both equations. For eq. (a), the maximum and minimum runoff variations can be observed in March 2008 and April 2006 with the ranges of 2.21 to 37 and 0 to 0.39, respectively (Fig. 9), whereas these values were 3.80 to 37.05 and 0 to 0.62 for eq. (b) (Fig. 10).

Additionally, the greatest and smallest variations occurred in March 2008 and April 2006, which these values varied from 8.61 to 38.77 and 0 to 0.62 by employing eq. (c), respectively (Fig. 11). The maximum percent values of runoff generated by rainfall events through eqs. (a), (b), and (c) were presented in Table 4. The results of eq. (a) indicated that the fraction of rainfall volume took part in runoff generation could vary from 7.25 to 72.79% while this participation could differ from 11.44 to 72.89% and 11.44 to 76.27% for eqs. (b) and (c), respectively.

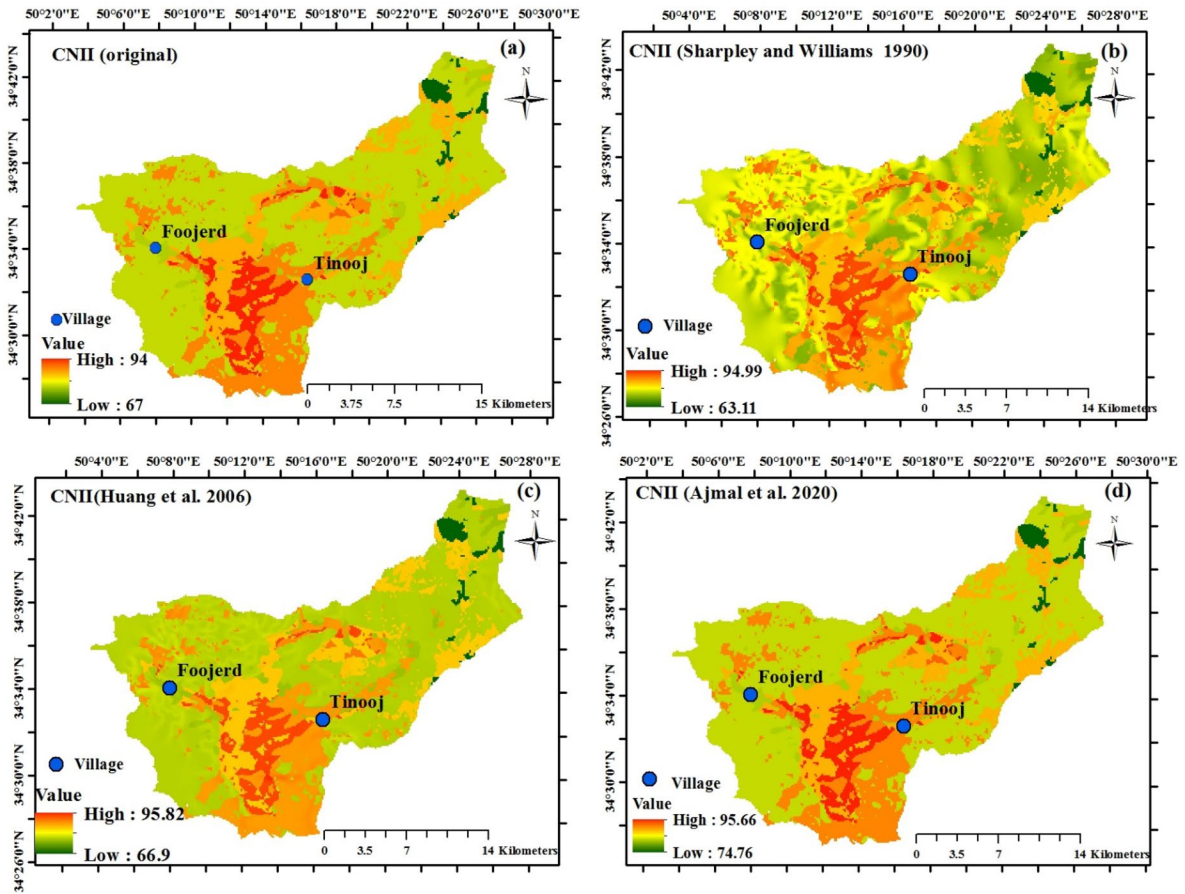


**Fig. 8** Curve number values of AMC-II condition with different equations

The average observed and estimated runoff for the mean rainfall event were calculated in Table 5. The observed runoff depth varied from 1 to 11.55 mm, while the mean rainfall volume ranges were 4.96 to

48.66 mm. The variations for estimated values of eqs. (a), (b), and (c) were 0.09 to 15.23, 0.01 to 16.48, and 0.033 to 21.91 mm.

**Table 3** The curve number classification area

CN values class	CNII (original) Area (%)	CNII (eq. a)	Change by eq. (a)	CNII (eq. b)	Change by eq. (b)	CNII (eq. c)	Change by eq. (c)
Less than 68	1.6	1.29	0.31 (decrease)	1.6	0	0	1.6 (decrease)
68–79	60.85	26.80	34.05 (decrease)	27.5	33.35 (decrease)	1.59	59.26 (decrease)
79–89	31.37	58.19	26.82 (increase)	57.15	25.78 (increase)	60.8	29.43 (increase)
89–100	6.18	13.72	7.54 (increase)	13.75	7.57 (increase)	37.61	31.43(increase)



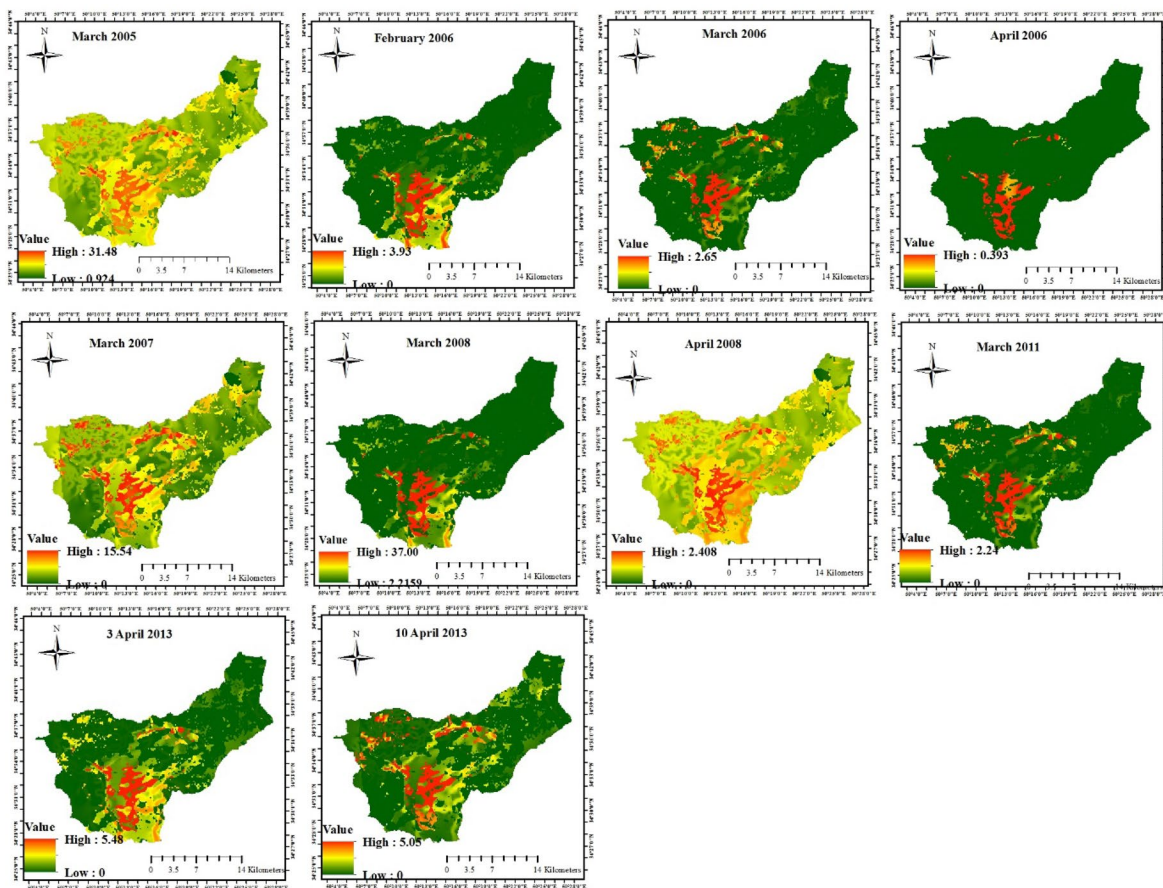


**Fig. 9** Spatio-temporal runoff maps (eq. a)

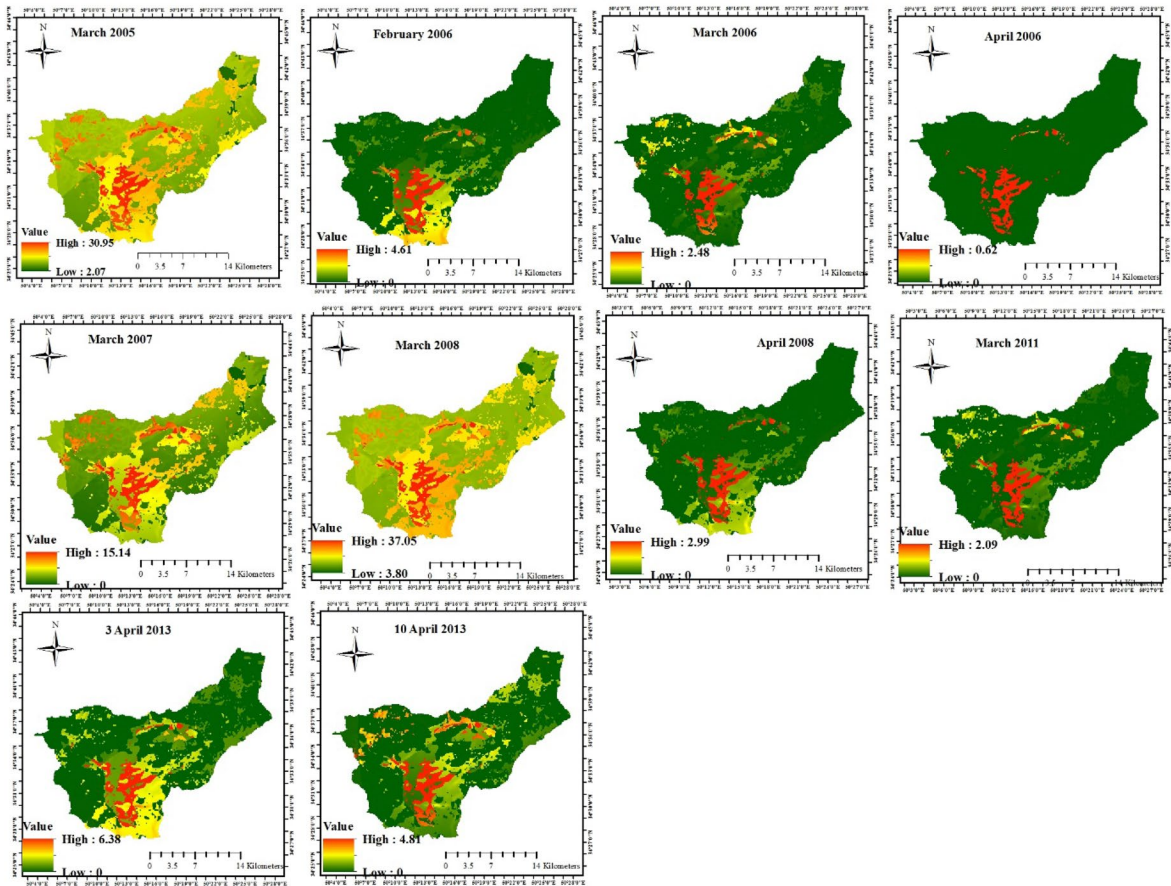
### Models performance evaluation

Table 6 showed the statistical indicator results for three models. The lower the RMSE value, the stronger the model performance. RMSE values for eqs. (a), (b), and (c) were 2, 2.30, and 3.74, respectively. On the basis of this statistical indicator, eq. (a) predicted runoff more accurately than the other equations. Also,  $E$  values of (a), (b), and (c) models were 0.78, 0.71, and 0.22, respectively. These values indicated very good, good, and unsatisfactory performance of three models. So, the best performance value was assigned to eq. (a). For percent bias (PB), the values between  $\pm 10$  and  $\pm 25$  showed the satisfactory model whereas  $-10 < PB < +10$  specified the model with very good performance (Moriassi et al., 2007; Ritter & Muñoz-Carpena, 2013). In this study, PB values for eqs. (a) and (b) revealed very good agreement between the

observed and predicted values while the value for eq. (c) indicated the satisfactory status. Additionally, high correlation between observed and estimated values,  $R^2$ , were observed for both models (0.88, 0.87, and 0.89).

### Discussion

Topography is known as a key factor for runoff estimation. This study tested the accuracy of three slope-adjusted CN ( $CN_{II}$ ) approaches for runoff prediction. The equation of Huang et al. (2006) which was proposed for 14 to 140% slopes indicated the satisfactory prediction for two indicators,  $E$  and  $R^2$ , and the unsatisfactory values for RMSE and PB indexes in this research. Although Shi and Wang (2020) reported the improvement in the large rainfall-runoff events



**Fig. 10** Spatio-temporal runoff maps (eq. b)

prediction of this equation at a higher slope of 0.90, the overestimated runoff of rainfall events which were more than 40 mm and underestimated runoff for rainfall events less than 40 mm could be observed in this study. The former research also verified limited improvement in its prediction for steep-slope watersheds (Ebrahimian et al., 2012; Shi & Wang, 2020). Another formula suggested by Ajmal et al. (2020) considered theoretical bounds of curve number (CN=0 and CN=100). This method not only overestimated and underestimated runoff the same as eq. (b) but also did not present the acceptable values for PB and RMSE indexes. This equation was proposed for the average slope of 7.50 to 53.53%, while the slope less than 5% could be seen in 51.60% in the watershed.

When Sharpley and Williams (1990) approach was applied, the computed runoff values were closer to the observed ones. Although the runoff results

showed the overestimation of large rainfall values and the underestimation for rainfall with less than 40 mm volume (Table 5), the values of  $E$  (0.78), RMSE (2), PB (16), and  $R^2$  (0.88) revealed that eq. (a) proposed by Sharpley and Williams (1990) was the most accurate model. The application of this method has been criticized because of testing with limited data (Huang et al., 2006), while its precision was approved by the acceptable results in recent studies (Deshmukh et al., 2013; Sujud & Jaafar, 2022; Verma et al., 2018).

It is obvious that correct runoff estimation in every region depends on assigning spatial rainfall and potential maximum retention parameter ( $S$ ). Curve number along with potential maximum retention parameters vary spatially due to slope, land use, and soil properties changes, which could be depicted through employing Arc-GIS. Applying the GIS and SCS-CN methods could specify the areas appropriate for water resource



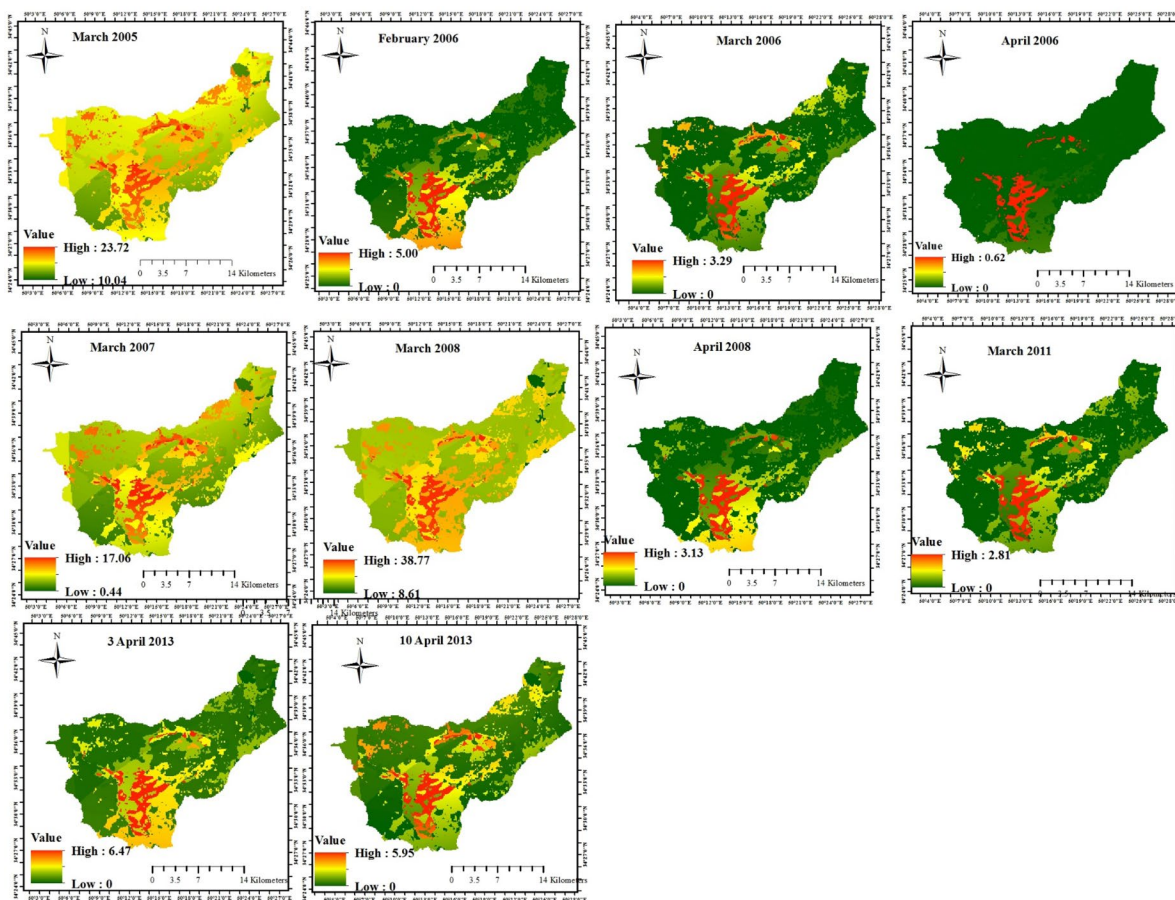


**Fig. 11** Spatio-temporal runoff maps (eq. c)

**Table 4** The maximum runoff generated by rainfall

No	Month/year	(% Maximum generated runoff by equation		
		(a)	(b)	(c)
1	March/2005	68.43	67.28	51.57
2	February/2006	29.44	34.53	37.45
3	March/2006	24.09	22.55	29.91
4	April/2006	7.25	11.44	11.44
5	March/2007	53.59	52.21	58.83
6	March/2008	72.79	72.89	76.27
7	April/2008	23.08	28.75	30.10
8	March/2011	22.40	20.90	28.10
9	3April/2013	36.48	42.48	43.08
10	10April/2013	33.67	32.07	39.67

management implementations such as rainwater harvesting in arid and semi-arid watersheds (Raghavan et al., 2022). As could be seen in Table 4 and Figs. 9, 10, and 11, the maximum percent of runoff generated by rainfall for eqs. (a), (b), and (c) were 68.43, 67.28, and 51.57%, respectively. The runoff potential could be attributed to rainfall, soil properties, slope, and land use. Figures 9, 10, and 11 showed that regardless of rainfall volume, the bareland with less than 15% slope covered with loam and clay loam textures, located in the south part of the watershed, was the most susceptible land to runoff generation and should be paid attention to surface water management. The runoff potential capability of this part was impressed by the reduction of soil infiltration rate, which caused lower

**Table 5** Mean observed and estimated runoff values

No	Month/year	Rainfall (mm)	Observed runoff (mm)	Estimated runoff by equation		
				(a)	(b)	(c)
1	March/2005	41.14	10.92	11.31	12.24	15.82
2	February/2006	10.925	1.01	0.27	0.292	0.6
3	March/2006	8.805	1.03	0.22	0.106	0.288
4	April/2006	4.96	1.14	0.09	0.01	0.033
5	March/2007	23.325	7.91	3.24	3.242	5.51
6	March/2008	48.66	11.55	15.23	16.48	21.91
7	April/2008	8.7	1.06	0.13	0.142	0.33
8	March/2011	8.565	1.00	0.09	0.097	0.26
9	3 April/2013	13.75	1.05	0.59	0.61	1.28
10	10 April/2013	12.01	1.04	0.35	0.359	0.87

maximum potential water retention. Furthermore, the minimum runoff generation in the northeast part could be attributed to rangelands with mild slope (0–5%) which have sandy loam and sandy clay loam soil textures. This research, like previous studies Tejram et al. (2012), Tirkey et al. (2014), Satheeshkumar et al. (2017) Al-Ghobari et al. (2020), Kumar et al. (2021), and Bera et al. (2022), confirms the effectiveness of the GIS-based SCS-CN model for temporal and spatial estimation of runoff which help water resource management.

As explained before, in addition to slope, runoff volume depends on intensity and duration of rainfall, which are significantly variable in arid regions. Therefore, it is suggested to test the modified equations of the SCS-CN approach which consider both parameters of slope and rainfall properties simultaneously. Finally, it should be noted that these results were restricted to one watershed which could be representative of the other watersheds in arid regions. So, it is proposed to test these approaches in other conditions to verify these achievements.

**Table 6** Statistical indicator results

Equation	<i>E</i>	RMSE	PB	<i>R</i> <sup>2</sup>
<i>a</i>	0.78	2.00	16	0.88
<i>b</i>	0.71	2.30	11	0.87
<i>c</i>	0.22	3.74	−24	0.89

### Conclusion

This study applied the combination of GIS and three methods of slope-adjusted curve number to compare the precision of these models for runoff prediction in the watershed located in the arid region. For this purpose, soil texture, hydrologic soil group, land use, slope, and daily rainfall volume maps were prepared in Arc-GIS. Land use map comprises rangeland, agricultural land, and bareland. The hydrologic soil group was built based on soil texture and classified into four classes, which its dominant class (B) comprises 68.95% of the watershed. The curve number map was provided for wet, normal, and dry conditions. Modifying the curve number values of normal condition, which varied from 67 in the agricultural land to 94 in the bareland areas based on three equations, caused the increase in CN values in most parts of the study area. The modified CN value maps showed that most of high CN values were at a slope of more than 10%. Consequently, spatial runoff maps were estimated for ten daily rainfall volumes from 2005 to 2013. Comparing the mean observed and estimated runoff with four performance indicators showed that the best agreement between observed and predicted runoff occurred with eq. (a) which was proposed by Sharpley and Williams (1990). The spatial runoff map was utilized to show sensitive lands and specify the fraction of rainfall volume that participated in runoff generation. So, the GIS-based approach helps

water resource decision makers to determine critical areas for runoff generation precisely. It is suggested to apply these models in other conditions to approve these obtained results.

**Acknowledgements** I would like to thank the natural resource and watershed management department and regional water office of Qom province for helping me to provide information for this research.

**Author contribution** All the stages of this study (collecting and analyzing hydrometric and climatic statistics, gathering and providing different layers in Arc-GIS, performing the methodology of the research, analyzing results, and finally writing this paper) were done by Elham Forootan.

**Data availability** If it is necessary, I will send used data.

## Declarations

**Ethics approval** Not applicable.

**Consent for publication** I sent this article for publishing in this journal.

**Conflict of interest** The author declares no competing interests.

## References

- Ajmal, M., Waseem, M., Ahn, J. H., & Kim, T. W. (2015). Improved runoff estimation using event-based rainfall-runoff models. *Water Resources Management*, 29(6), 1995–2010.
- Ajmal, M., Waseem, M., Ahn, J. H., & Kim, T. W. (2016). Runoff estimation using the NRCS slope-adjusted curve number in mountainous watersheds. *Journal of Irrigation and Drainage Engineering*, 142(4), 04016002.
- Ajmal, M., Waseem, M., Kim, D., & Kim, T. W. (2020). A pragmatic slope-adjusted curve number model to reduce uncertainty in predicting flood runoff from steep watersheds. *Water*, 12(5), 1469.
- Al-Ghobari, H., Dewidar, A., & Alataway, A. (2020). Estimation of surface water runoff for a semi-arid area using RS and GIS-based SCS-CN method. *Water*, 12(7), 1924.
- Auerswald, K., & Gu, Q. L. (2021). Reassessment of the hydrologic soil group for runoff modelling. *Soil and Tillage Research*, 212, 105034.
- Bera, D., Kumar, P., Siddiqui, A., & Majumdar, A. (2022). Assessing impact of urbanisation on surface runoff using vegetation-impervious surface-soil (VIS) fraction and NRCS curve number (CN) model. *Modeling Earth Systems and Environment*, 8(1), 309–322.
- Bhuyan, M. J., Borah, D., Nath, B. K., Deka, N., & Bora, A. K. (2022). Runoff estimation of the Kolong River Basin in Assam, India using NRCS-curve number method and geospatial techniques. In *Drainage basin dynamics* (pp. 441–453). Springer, Cham.
- Chaplot, V. A., & Le Bissonnais, Y. (2003). Runoff features for interrill erosion at different rainfall intensities, slope lengths, and gradients in an agricultural loessial hillslope. *Soil Science Society of America Journal*, 67, 844–851.
- Chaudhary, A., Mishra, S. K., & Pandey, A. (2013). Experimental verification of effect of slope on runoff and curve numbers. *Journal of Indian Water Resources Society*, 33, 40–46.
- Deshmukh, D. S., Chaube, U. C., Hailu, A. E., Gudeta, D. A., & Kassa, M. T. (2013). Estimation and comparison of curve numbers based on dynamic land use land cover change, observed rainfall-runoff data and land slope. *Journal of Hydrology*, 492, 89–101.
- Ebrahimian, M., Nuruddin, A. A. B., Soom, M. A. B. M., Sood, A. M., & Neng, L. J. (2012). Runoff estimation in steep slope watershed with standard and slope-adjusted curve number methods. *Polish Journal of Environmental Studies*, 21(5), 1191–1202.
- Evelt, S. R., & Dutt, G. R. (1985). Length and slope effects on runoff from sodium dispersed, compacted earth micro-catchments. *Soil Science Society of America Journal*, 49, 734–738.
- Fang, H. Y., Cai, Q. G., Chen, H., & Li, Q. Y. (2008). Effect of rainfall regime and slope on runoff in a Gullied Loess region on the Loess Plateau in China. *Journal of Environmental Management*, 42(3), 402–411.
- Farran, M. M., & Elfeki, A. M. (2020). Statistical analysis of NRCS curve number (NRCS-CN) in arid basins based on historical data. *Arabian Journal of Geosciences*, 13(1), 1–15.
- Forootan, E. (2019). Analysis of trends of hydrologic and climatic variables. *Soil and Water Research*, 14(3), 163–171.
- Geena, G. B., & Ballukraya, P. N. (2011). Estimation of runoff for Red hills watershed using SCS method and GIS. *Indian Journal of Science and Technology*, 4, 899–902.
- Gitika, T., & Ranjan, S. (2014). Estimation of surface runoff using NRCS curve number procedure in Buriganga Watershed, Assam, India-A geospatial approach. *International Research Journal of Earth Sciences*, 2, 1–7.
- Gonzalez, A., Temimi, M., & Khanbilvardi, R. (2015). Adjustment to the curve number (NRCS-CN) to account for the vegetation effect on hydrological processes. *Hydrological Sciences Journal*, 60(4), 591–605.
- Gupta, L., & Dixit, J. (2022). Estimation of rainfall-induced surface runoff for the Assam region, India, using the GIS-based NRCS-CN method. *Journal of Maps*, 1–13.
- Hawkins Richard, H. (2014). Curve number method: Time to think anew? *Journal of Hydrologic Engineering*, 19, 1059.
- Huang, M., Gallichand, J., Wang, Z., & Goulet, M. (2006). A modification to the Soil Conservation Service curve number method for steep slopes in the Loess Plateau of China. *Hydrological Processes: An International Journal*, 20(3), 579–589.
- Ibrahim, S., Brasi, B., Yu, Q., & Siddig, M. (2022). Curve number estimation using rainfall and runoff data from five catchments in Sudan. *Open Geosciences*, 14(1), 294–303.
- Jha, R. K., Mishra, S. K., & Pandey, A. (2014). Experimental verification of effect of slope, soil, and AMC of a fallow land on runoff curve number. *Journal of Indian Water Resources Society*, 2014(34), 40–47.

- Kang, M., & Yoo, C. (2020). Application of the SCS-CN method to the Hancheon basin on the volcanic Jeju Island, Korea. *Water*, 12(12), 3350.
- Kumar, A., Kanga, S., Taloor, A. K., Singh, S. K., & Āurin, B. (2021). Surface runoff estimation of Sind river basin using integrated SCS-CN and GIS techniques. *HydroResearch*, 4, 61–74.
- Mahmood, K., Qaiser, A., & Farooq, S. (2020). RS- and GIS-based modeling for optimum site selection in rain water harvesting system: An SCS-CN approach. *Acta Geophysica*, 68(4), 1175–1185.
- Mishra, S. K., Chaudhary, A., Shrestha, R. K., Pandey, A., & Lal, M. (2014). Experimental verification of the effect of slope and land use on SCS runoff curve number. *Water Resources Management*, 28, 3407–3416.
- Mishra, S. K., Geetha, K., Rastogi, A. K., & Pandey, R. P. (2005). Long-term hydrologic simulation using storage and source area concepts. *Hydrological Processes: An International Journal*, 19(14), 2845–2861.
- Moriassi, D. N., Arnold, J. G., Van Liew, M. W., Bingner, R. L., & Harmel, R. D. (2007). Veith TL (2007) Model evaluation guidelines for systematic quantification of accuracy in watershed simulations. *Transactions of the ASABE*, 50, 885–900.
- Natural Resource, & Watershed Management Department of Qom province. (2010). Hydrology report. Qom, Iran.
- Nayak, T. R., & Jaiswal, R. K. (2003). Rainfall-runoff modelling using satellite data and GIS for Bebas River in Madhya Pradesh. *Journal of The Institution of Engineers (India)*, 84, 47–50.
- Nazif, S., Soleimani, P., Eslamian, S. (2022). Dynamic curve numbers: Concept and application. In Flood Handbook (pp. 357–384). CRC Press.
- NRCS, USDA. (2004). National engineering handbook: Part 630—Hydrology. Chapter 9: Hydrologic Soil-Cover Complexes. *United States Department of Agriculture-Natural Resources Conservation Service*.
- Philip, J. R. (1991). Hillslope infiltration: Planar slopes. *Water Resources Research*, 27, 109–117.
- Raghavan, R., Rao, K. V., Shirahatti, M. S., Srinivas, D. K., Reddy, K. S., Gopinath, C. G. R., & KA, Osman M, Prabhakar M, Singh VK., (2022). Assessment of spatial and temporal variations in runoff potential under changing climatic scenarios in northern part of Karnataka in India using geospatial techniques. *Sustainability*, 14(7), 3969.
- Rajbanshi, J. (2016). Estimation of runoff depth and volume using NRCS-CN method in Konar Catchment (Jharkhand, India). *Journal of Civil and Environmental Engineering*, 6(10.4172).
- Ritter, A., & Mu'noz-Carpena, R. (2013). Performance evaluation of hydrological models: Statistical significance for reducing subjectivity in goodness-of-fit assessments. *Journal of Hydrology*, 480, 33–45.
- Satheeshkumar, S., Venkateswaran, S., & Kannan, R. (2017). Rainfall-runoff estimation using SCS-CN and GIS approach in the Pappiredipatti watershed of the Vaniyar sub basin, South India. *Modeling Earth Systems and Environment*, 3(1), 1–8.
- Saxton, K. E., Rawls, W., Romberger, J. S., & Papendick, R. I. (1986). Estimating generalized soil-water characteristics from texture. *Soil Science Society of America Journal*, 50, 1031–1036.
- SCS. (1985, 1993, 2004). National engineering handbook section 4: Hydrology, chapter 4. Soil Conservation Service. Washington, DC: USDA.
- Sharma, I., Mishra, S. K., & Pandey, A. (2022). Can slope adjusted Curve Number models compensate runoff underestimation in steep watersheds?: A study over experimental plots in India. *Physics and Chemistry of the Earth, Parts A/B/C*, 103185.
- Sharpley, A. N., & Williams, J. R. (1990). EPIC—erosion/productivity impact calculator: 1. Model documentation. Washington, DC: US Government Printing Office, USDA Technical Bulletin No. 1768.
- Shi, W., & Wang, N. (2020). An improved SCS-CN method incorporating slope, soil moisture, and storm duration factors for runoff prediction. *Water*, 12(5), 1335.
- Singh, P. K., Mishra, S. K., Berndtsson, R., Jain, M. K., & Pandey, R. P. (2015). Development of a modified SMA based MSCS-CN model for runoff estimation. *Water Resources Management*, 29(11), 4111–4127.
- Soulis, K. X. (2021). Soil conservation service curve number (SCS-CN) method: Current applications, remaining challenges, and future perspectives. *Water*, 13(2), 192.
- Soulis, K. X., & Valiantzas, J. D. (2013). Identification of the SCS-CN parameter spatial distribution using rainfall-runoff data in heterogeneous watersheds. *Water Resources Management*, 27(6), 1737–1749.
- Sujud, L. H., & Jaafar, H. H. (2022). A global dynamic runoff application and dataset based on the assimilation of GPM, SMAP, and GCN250 curve number datasets. *Scientific Data*, 9(1), 1–11.
- Tejram, N., Verma, M. K., & Hema, B. S. (2012). SCS curve number method in Narmada basin. *International Journal of Geomatics and Geosciences*, 3, 219–228.
- Tirkey, A. S., Pandey, A. C., & Nathawat, M. S. (2014). Use of high-resolution satellite data, GIS and NRCS-CN technique for the estimation of rainfall-induced run-off in small catchment of Jharkhand India. *Geocarto International*, 29(7), 778–791.
- USDA. (1986). Urban hydrology for small watersheds, TR-55, United States Department of Agriculture, 210-VI-TR-55, 2nd edn June 1986.
- USDA, SCS. (1987). Soil mechanics level 1, Module 3-USDA Textural Classification. *US Department of Agriculture: Soil Conservation Service*.
- USDA-SCS, S. C. S. (1972). National engineering handbook. Section 4: hydrology, soil conservation service.
- Verma, R. K., Pandey, A., & Mishra, S. K. (2022). Curve numbers computation using observed rainfall-runoff data and RS and GIS-based NRCS-CN Method for direct surface runoff estimation in Tilaiya catchment. In *Geospatial Technologies for Land and Water Resources Management* (pp. 237–254). Springer, Cham.
- Verma, S., Singh, A., Mishra, S. K., Singh, P. K., & Verma, R. K. (2018). Efficacy of slope-adjusted curve number models with varying initial abstraction coefficient for runoff estimation. *International Journal of Hydrology Science and Technology*, 8(4), 317–338.

- Verma, S., Verma, R. K., Mishra, S. K., Singh, A., & Jayaraj, G. K. (2017). A revisit of NRCS-CN inspired models coupled with RS and GIS for runoff estimation. *Hydrological Sciences Journal*, 62(12), 1891–1930.
- Werner, J., Woodward, D. E., Nielsen, R., Dobos, R., Hjelmfelt, A., & Hoeff, C. C. (2007) Part 630 Hydrology national engineering handbook Chapter 7: Hydrologic soil groups. Report. United States Department of Agriculture.
- Willard, A. (2010). Hydrologic soil grouping determination for Appalachian minesoils. West Virginia University.
- Williams, J., Kannan, N., Wang, X., Santhi, C., & Arnold, J. (2012). Evolution of the SCS runoff curve number method and its application to continuous runoff simulation. *Journal of Hydrologic Engineering*, 17, 1221–1229.
- Williams, J. R., & Izaurralde, R. C. (2005). The APEX model. Temple, TX: Texas A&M Blackland Research Center, BRC Report no. 2005–2.
- Wood, M. K., & Blackburn, W. H. (1984). An evaluation of the hydrologic soil groups as used in the SCS runoff method on rangelands 1. *JAWRA Journal of the American Water Resources Association*, 20(3), 379–389.
- Yousuf, A., Bhardwaj, A., & Yousuf, F. (2022). Development and evaluation of GIS-based runoff and sediment yield watershed scale model. *Arabian Journal of Geosciences*, 15(19), 1–15.
- Zhan, X., & Huang, M. L. (2004). ArcCN-Runoff: An ArcGIS tool for generating curve number and runoff maps. *Environmental Modelling & Software*, 19, 875–879.
- Zhao, W. W., Fu, B. J., Chen, L. D., Zhang, Q. J., & Zhang, Y. H. (2004). Effects of land-use pattern change on rainfall-runoff and runoff-sediment relations: A case study in Zichang watershed of the Loess Plateau of China. *Journal of Environmental Sciences*, 16(3), 436–442.

**Publisher's Note** Springer Nature remains neutral with regard to jurisdictional claims in published maps and institutional affiliations.

Springer Nature or its licensor (e.g. a society or other partner) holds exclusive rights to this article under a publishing agreement with the author(s) or other rightsholder(s); author self-archiving of the accepted manuscript version of this article is solely governed by the terms of such publishing agreement and applicable law.